Preparation of ZnO/graphene heterojunction via high temperature and its photocatalytic property

**Delong Li · Wenhui Wu · Yupeng Zhang ·
Liangliang Liu · Chunxu Pan**

Abstract This paper introduces a novel electrochemical route for preparing the ZnO/graphene heterojunction composite via high temperature. This process includes: (1) depositing the electrochemically reduced graphene oxide (ERGO) on ITO glass via cyclic voltammetry; (2) pulse plating a zinc (Zn) layer on the ERGO; (3) thermally treating the Zn/ERGO composite and "in situ" to obtain the ZnO/ERGO composite. SEM characterizations revealed that the Zinc Oxide (ZnO) particles were homogenously distributed on the surface of graphene sheets. XRD and Raman spectra found a $ZnCO_3$ phase in the ZnO/ERGO composite, which demonstrated that when the Zn film transformed into ZnO particles during thermal treatment, Zn also reacted with graphene and formed a $ZnCO_3$ intermediate layer at the interface between ZnO and ERGO via short-range diffusion. Compared with the heterojunction formed from regular chemical route, the present process provided a tight contact and combination between ZnO and ERGO, which eventually led to a heterojunction between ZnO and graphene sheets. This heterojunction exhibited great improvement for separation efficiency of photo-generate electron–hole pairs. Experimental results of ultraviolet–visible (UV–Vis) light catalysis demonstrated that the photocatalytic activity of the ZnO/ERGO composite had been greatly improved, and exhibited a value of three times higher than that of pure ZnO.

D. Li · W. Wu · Y. Zhang · L. Liu · C. Pan
School of Physics and Technology, and MOE Key Laboratory of Artificial Micro- and Nano-structures, Wuhan University, Wuhan 430072, China

C. Pan
Center for Electron Microscopy, Wuhan University, Wuhan 430072, China

C. Pan (✉)
Department of Materials Physics, School of Physics and Technology, Wuhan University, Wuhan 430072, Hubei, China
e-mail: cxpan@whu.edu.cn

Introduction

Graphene is another allotrope of carbon besides fullerenes and CNTs, which could be considered a two-dimensional (2D) single or several atomic layers of graphite. It has been widely investigated due to its unique physical, chemical, and mechanical properties. Graphene based composite nano materials have attracted wide attention in the past few years [1, 2]. Besides, researchers also have noted that when inorganic materials, such as ZnO and TiO_2 are integrated with graphene, their properties will be greatly improved [1–5].

Oxide semiconductors have attracted wide attention due to the potential applications in areas such as photocatalyst, solar cell, and optoelectronic, etc. In addition to TiO_2 based photocatalyst [4–8], ZnO and its composite also attracted extensive attention [3, 9]. ZnO is a direct band gap semiconductor with a 3.3 eV band gap. Due to its unique optical and electrical properties with various morphologies, ZnO has been widely used in solar cell, photocatalyst, and piezoelectric materials [10]. However, its applications are still limited because of its inherent defects involving wide band gap, which restricts the absorbing wavelength no longer than 375 nm just in the ultraviolet light range and results in low light utilization efficiency. In order to overcome these disadvantages, integrating ZnO with graphene to fabricate composite is a simple and efficient method. The excellent properties of graphene contribute to the preparation of high efficiency photocatalyst.

Recently, several kinds of ZnO/graphene composites have been reported [11–19]. The performances of the composites are different due to the variant preparation

methods, which have been widely used in different ZnO morphologies including nano-needle, nano-rod, nano-wire, and nano flower, etc. Kim et al. [11] prepared the vertical ZnO nanoneedle arrays on graphene sheets through catalyst-free metal–organic vapor-phase epitaxy. It was found that the completed array structure only grown on the graphene sheet substrate, and the Photoluminescence characteristics of ZnO nanostructure on graphene layer were almost the same to those of pure ZnO nanostructure, which suggested that ZnO nanostructures grown on the graphene layers without deterioration of the graphene layer during preparation. Hwang et al. [12] prepared ZnO/graphene composite from hydrothermal process. The ZnO nanowires grown on the reduced graphene film, which exhibited an excellent field emission property. Lin et al. [13] synthesized the ZnO/graphene heterogeneous nanostructures via chemical vapor deposition (CVD). It was observed that the morphology of ZnO changed from nanorod into micro-nano-needle with the increase of temperature, which showed an excellent optical property.

ZnO/graphene nano-composite also showed a great potential application in electrochemical supercapacitors. This nano-composite could be prepared via variant processes, such as microwave assisted reduction of zinc ions in aqueous solution with graphite oxide dispersion, [14] and ultrasonic spray pyrolysis method. [13] The composites exhibited an enhanced capacitive behavior through better reversible charging/discharging ability and higher capacitive values by comparison with pure ZnO or graphene electrode. Alternate preparations include the graphene coated ZnO via plasma-enhanced CVD and CVD method, [16] and direct depositing ZnO on the surface of graphene, were prone to solar cell applications [17].

In the field of photocatalysis, Li et al. [18] prepared the ZnO/graphene composite photocatalyst with high photocatalytic activity via the chemical deposition. Xu et al. [19] prepared the ZnO/graphene composite by restoring the oxidized graphene. The photocatalytic property of the composite was improved to some extent by depredating methylene. According to these studies, the reason for improving photocatalytic efficiency is the interaction of ZnO particles and graphene sheets, which increases the electron transmission speed and inhibits the electron–hole recombination [18, 19].

It has been well-known that a crucial point for obtaining a high-quality composite system is to achieve a tight contact interfaces between different phases, i.e. to form a heterojunction structure. In general, the preparation of ZnO/graphene composites whether via hydrothermal or mechanical stirring were both at relatively low temperature, which might result in a simple and loose interaction at the interface between ZnO and graphene sheet. That is to say, there might be a "gap" at the interface or no real heterojunction formed

due to the "virtual contact". Obviously, this phenomenon will restrict the ZnO/graphene composites to lower level of photocatalytic property and also lead to the instability.

In this paper, we introduce a novel route to prepare the ZnO/graphene composite via following process: firstly, synthesizing a graphene layer on a conductive glass via electrochemical process [20]; secondly, depositing a layer of zinc (Zn) film on the graphene by using a pulse electrodeposition; and finally, in situ oxidizing the Zn film to ZnO through high-temperature thermal oxidation [21]. When Zn transformed to ZnO at high temperature, the short range atomics interdiffusion happened between ZnO and graphene, which induced a transition layer at the interface, i.e. formed a heterojunction interface. Obviously, this is a real heterojunction and advantage to increase the photo-induced electron–hole separation efficiency [9].

Experimental section

Preparation of the ZnO/graphene composite was according to the following process: (1) Took appropriate amount of graphene oxide which was prepared from modified hummers method [22], and dispersed it into distilled water and keep the solubility of the aqueous solution of oxidized graphene at 1 mg/ml. (2) Deposited the graphene on the ITO glass was carried out in a three-electrode system (Platinum plate as the counter electrode, HgI as the reference electrode, and ITO glass as the working electrode platinum) by cyclic voltammetry, the initial voltage was 0 V, and the scan speed was 0.1 v/s. The high voltage was 0 V and the low voltage was −1.5 V. The number of cycles was five. (3) After graphene electrode was prepared, Zn nanocrystalline layer was plated upon the surface of ERGO using square wave pulse plating process. The main composition of the electrolyte was $ZnCl_2$. The anode was Zn foil with 99.9 % purity, and the cathode was ERGO on ITO substrate with 10 s pulsed plating, the PH value of the electrolyte was 5.0, which can be adjusted by adding hydrochloric acid (HCl) and potassium hydroxide (KOH). During the 10 s pulse plating process, the forward voltage was 3.0 V, reverse voltage was 1.0 V, and duty cycle was 40 %. (4) Cleaned the conductive glasses, and removed the inorganic salt in the electrolyte. (5) At last, the Zn/ERGO composite was heated at 350 °C for 2 h in the air to oxide Zn into ZnO, as shown in Fig. 1.

Phase structure of the ZnO/graphene composite was tested by X-ray diffraction (XRD) (D8 Advanced XRD, Bruker AXS, Karlsruhe, Germany) with parameters including tube voltage of 40 kV, tube current of 40 mA, and CuKα radiation (the incident wavelength is λ = 0.15406 nm). Morphologies and microstructures of the ZnO/graphene composite were characterized by using field-emission gun scanning electron microscope (SEM) (S-4800, Hitachi High-
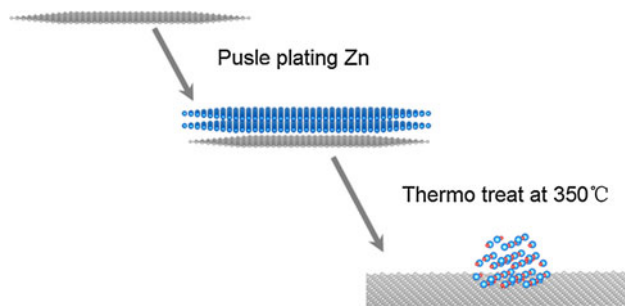
Fig. 1 The process for preparing the ZnO/graphene composite

Technologies Corporation, Japan). Raman spectra of the composite were measured in a laser scanning confocal micro-Raman spectrometer (LabRAM HR, HORIBA, France).

The photocatalytic activity of the ZnO/ERGO composite was measured by detecting the concentration variety of ·OH generated in the terephthalic acid (TA) solution under the ultraviolet–visible (UV–Vis) irradiation, which was conducted according to the literature [23, 24]. The composite was entirely immersed in 3 mL aqueous solution containing 10 mM NaOH and 3 mM TA. Before exposure to the visible light irradiation, the solution was left in the dark for 30 min. Then it was irradiated perpendicularly by a 450 W high pressure mercury lamp. The fluorescence signal of the 2-hydroxy terephthalic acid (TAOH) was measured in situ every half hour by using a fluorescence spectrophotometer (F-4500, Hitachi, Japan) with the excitation light from a Xe lamp. The excitation light employed in recording fluorescence spectra was 320 nm.

The intensity of photo-generated current was measured by electrochemical workstation (CHI660C, Chenhua, Shanghai, China). The prepared samples, saturation calomel electrode, and platinum electrode were used as the working electrode, reference electrode, and counter electrode, respectively. They were all immersed in 0.1 M Na_2SO_4 aqueous solution together. The working electrode 1 cm^2 films were irradiated horizontally by a 150 W high pressure mercury lamp, which generate light wavelength in the range of 350–450 nm. The distance between the lamp and electrode was 10 cm.

Results and discussion

Figure 2 shows SEM morphologies of the ZnO/graphene composite in different stages of preparation. It can be seen that the graphene distributed smoothly on the conductive glass and the pulse electro-deposited Zn film homogeneously covered on the graphene surface. After heat treatment, it was found that the original Zn film shrank into granular particles. Raman spectroscopy, as shown in Fig. 3a, had a strong G peak and relatively weak and broaden 2D peak of the original graphene via cyclic voltammetry, which revealed that it had a lot of defects. However, after thermal oxidation of the composite, in addition to the characteristic peak of graphene, the characteristic E_2 and E_1 peaks of ZnO at 434 and 587 cm^{-1} was also observed [25], as shown in Fig. 3b, which indicated the formation of the ZnO/graphene composite.

Figure 4 illustrates the XRD patterns of the ZnO/graphene composite in different stages of preparation, respectively. It was found that in addition to the transformation of Zn into ZnO during thermal oxidation, a $ZnCO_3$ phase was also observed. The existence of the intermediate $ZnCO_3$ phase demonstrated that an interdiffusion and interaction of carbon and Zn atoms occurred at the interface during the oxidization of Zn to ZnO progress, due to good lattice matching between Zn and graphene during high-temperature thermal oxidation.

It was this intermediate phase which achieved a tight contact of ZnO with ERGO, that is to say, a heterojunction formed between ZnO and ERGO in the composite. This was of significant importance for the electron transfer between ZnO and ERGO, and exhibited a great improvement of the separation efficiency of the photogenerated electron–holes. However, due to the limitations of experimental conditions, the HRTEM image at the interface of ZnO and graphene can hardly be observed; and since content of ERGO was rarely small, the XRD results could also hardly detect the interface.

We believed that the heterojunction between ZnO and ERGO was formed during heat treatment, due to the interdiffusion of carbon and zinc. The thickness of the diffusion layer could be simply calculated from the Fick's
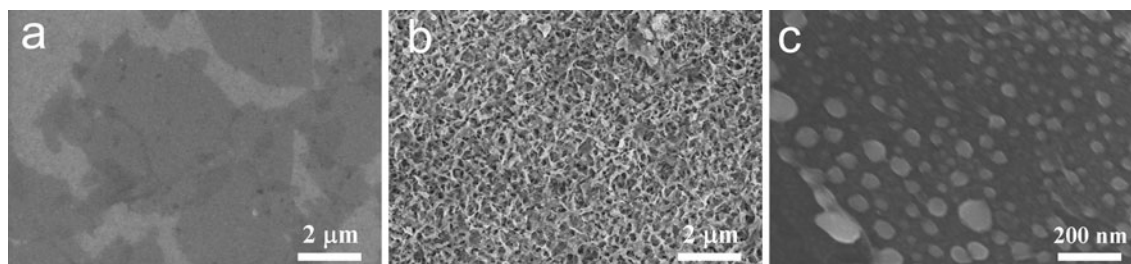

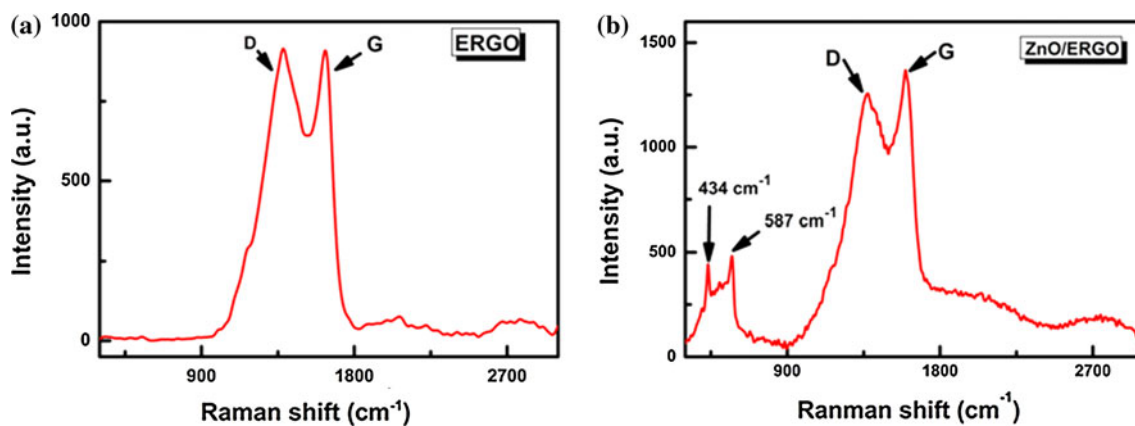Fig. 2 SEM morphologies of the samples. (a) ERGO, (b) Zn/ERGO, (c) ZnO/ERGO

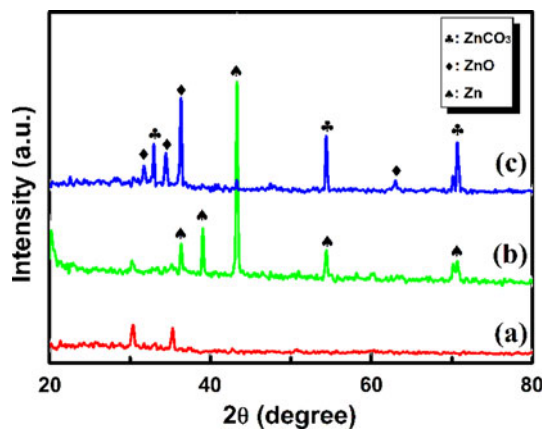Fig. 3 Raman spectra of the samples. (a) ERGO, (b) ZnO/ERGO

Fig. 4 XRD patterns of the samples on ITO glass. (a) ERGO, (b) Zn/ERGO, (c) ZnO/ERGO

second law. Actually, at the interface, high temperature provided enough energy for active carbon atoms diffusing into the Zn plating and forming a solid solution. At the same time, an oxidation reaction of the Zn layer happened due to the surplus O_2 in the atmosphere, which resulted in a phase transformation from Zn into ZnO. Also, the Diffusion layer of Zn and C had captured O_2 and transformed into a $ZnCO_3$ transitional layer.

Considering the C diffusing in Zn, a calculation based on the Fick's law was performed according to a simple one-dimensional model. At the beginning, it was assumed that the C concentration was 100 %, and after the diffusion, the proportions of C and Zn matched the atomic ratio in $ZnCO_3$, i.e., $C_c\% = 15.58$ %.

The initial conditions were $t = 0$ and $C_c = C_0$, where C_0 was the original C concentration of the Zn plating, considered as $C_0 = 0$. The boundary conditions were at $t > 0$ and $x = 0$, $C_c = Cs = 1$ and $X = \infty$, $C_c = 15.58$ %. According to the Fick's law, it was calculated that:

$$C_c = Cs - (Cs - C_0)\mathrm{erf}\left(x/2\,(Dt)^{1/2}\right) \tag{1}$$

From above conditions, the error function was erf ($x/2$ $(Dt)^{1/2}$) = erf (β) = 84.42 %, referring to graph $\beta = 1$. Therefore, the diffusion depth of C in Zn was

$$x = 2\,(Dt)^{1/2} \tag{2}$$

The diffusion of C in Zn belonged to a kind of interstitial diffusion mechanism, and the diffusion coefficient could be calculated from the formula $D = D_0\exp(-Q/RT)$. According to the literature [26], $D_0 = 1 \times 10^{-5}$ cm^2/s and $Q = 50{,}200$ cm^2/s, and consequently, the variations of the diffusion depth with time at different temperatures were obtained, as shown in Fig. 5. This simple simulation just indicated the diffusion phenomenon happened during heat treatment in the present case. Practically, there were many factors that influenced the interdiffusion of C and Zn, such as carbon concentration, grain boundaries, defects, etc. Therefore, the actual diffusion depth was much smaller than those determined from the calculations. However, with high temperature, the tight contact heterojunction can be observed, and the diffusion interface formed due to the short range atom diffusion at the interface [9, 27].

In our previous study, it was found that the electro-deposited Zn layer was transformed into ZnO-nanoneedles during thermal oxidation, which was considered to be a growth mechanism of "solid state based-up diffusion model" [21]. However, in this study, due to the short time plating and thin Zn film (only a few microns), the Zn film tended to be transformed into liquid phase with large surface tension during thermal treatment, which inhibited ZnO growth in a preferred orientation according to the above model, and finally, the ZnO grew as a kind of irregular particles. In addition, the reinforced surface energy of graphene sheets was also prone to form the particles during Zn shrinking on the surface. Obviously, the shape of ZnO particle was different from the typical hexagonal structure of ZnO nanorods, but it was also reported in literature [18].
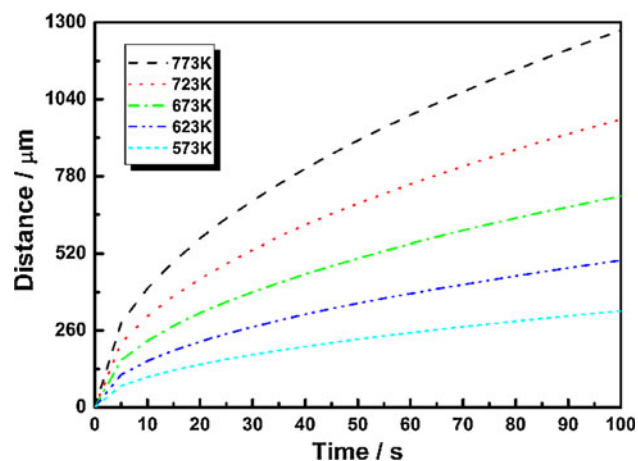
Fig. 5 Relationships of diffusion depth with time at different temperatures

It is well-known that Fluorescence spectra is an efficient method to evaluate photocatalytic activity by measuring the formation and variety of photocatalytic active species ·OH radicals under the UV–Vis light irradiation. TA was used as the fluorescence probe because it reacted with ·OH in solution to generate TAOH. With the 320 nm excitation light irradiation, TAOH emitted a unique fluorescence signal with a peak at 426 nm and its intensity variation was coincident with concentration. Thus, the concentration of hydroxyl radical (·OH) could be measured from the variations of fluorescence intensity of the solution. The detailed procedure is as follows:

$$ZnO + h \rightarrow e^- + h_{vb} \tag{3}$$

$$OH- + h_{vb} \rightarrow OH· \tag{4}$$

$$TA + OH· \rightarrow TAOH \tag{5}$$

The photocatalytic property of the ZnO/ERGO composite film was characterized by using a UV–Vis light irradiation catalyzing TA. The fluorescence spectra associated with TAOH were generated by irradiating the ZnO/ERGO, as shown in Fig. 6. The result demonstrated that after photodegradation for 3 h, the photocatalytic efficiency of the ZnO/ERGO composite increased approximately three times higher than that of ZnO. The inset of Fig. 6 is photodegradation curves of the ZnO/graphene, ZnO, and graphene, respectively. From comparison, it could be seen that while graphene had no photodegradation effect, and ZnO exhibited a strong photocatalytic activity, the composite enhanced and almost tripled the photocatalytic efficiency.

In fact, this enhancement for photocatalytic property mainly came from the improvement of the photogenerated electron -holes separation efficiency. Fig. 7 shows the fluorescence curves of the ZnO and ZnO/graphene composite. In general, ZnO exhibits a strong fluorescence property. For the
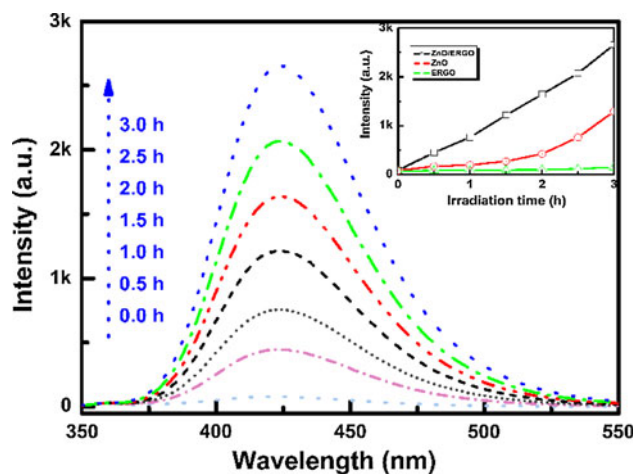

Fig. 6 Fluorescence spectra obtain for the supernatant liquid of the irradiated ZnO/ERGO solution containing 3mMTA at various irradiation periods, and the inset is the time dependence of fluorescence intensity at 426 nm of ERGO, ZnO, and ZnO/ERGO composite
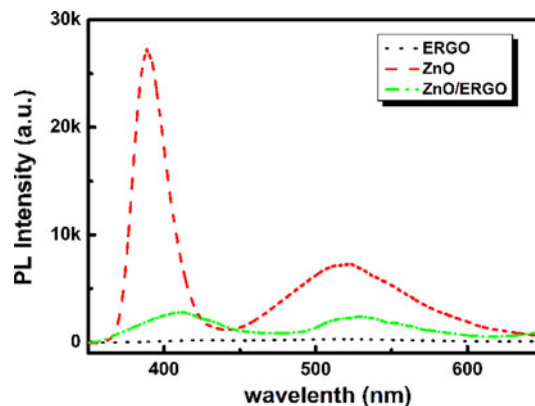

Fig. 7 Fluorescence spectra of ERGO, ZnO, and ZnO/ERGO composite

present case, the ZnO prepared from thermal oxidation also showed strong fluorescence intensity, and the defect peak was obvious too, due to the heat treatment in the air. However, for the composite, the fluorescence intensity decreased greatly, as shown in Fig. 7, which proved that the recombination efficiency of photogenerated electron-holes reduced significantly under the excitation light.

Figure 8 illustrates the photocurrent curves of pure ZnO and the ZnO/ERGO composite. Obviously, the photocurrent intensity of the ZnO/ERGO composite was about two times higher than that of pure ZnO, and the photocurrent intensity of the ERGO was almost negligible, when compared with ZnO or ZnO/ERGO composite. The photocurrent provided a direct characterization of photocatalytic activity of the composite, which revealed the photo-generated electron-hole pairs under the UV–Vis light irradiation.
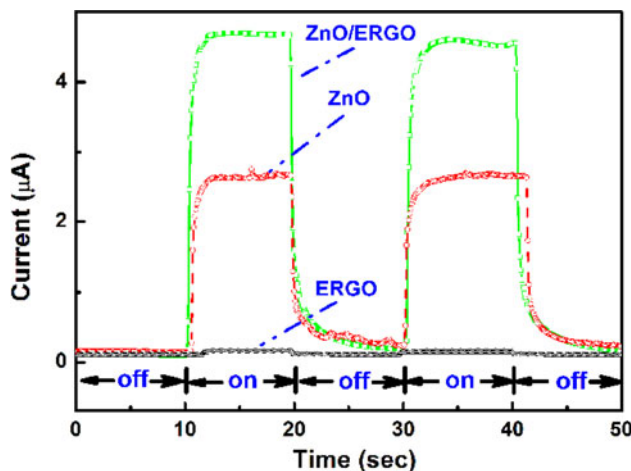
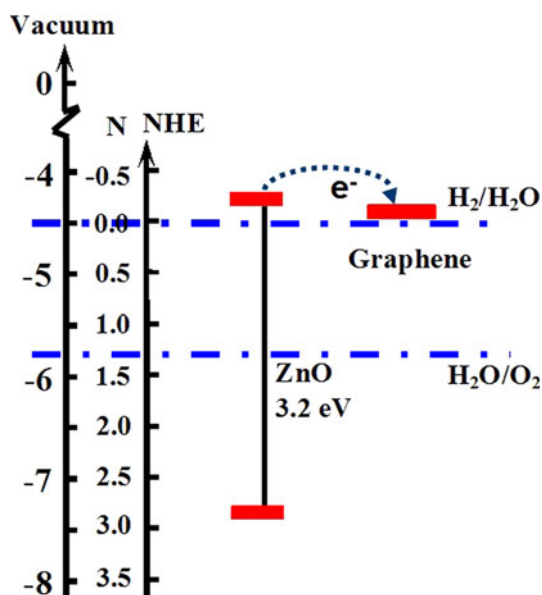**Fig. 8** Photocurrent of ZnO and ZnO/ERGO composite

Fig. 9 Energy band structure of ZnO and graphene

Figure 9 shows the energy level diagram of ZnO and graphene. It can be seen that the conduction band position of ZnO is higher than that of graphene, which resulted in the movement of electrons from ZnO to graphene. Therefore, theoretic analysis revealed that, due to the advantages of the heterojunction at the interface between ZnO and graphene, and the extremely excellent electron mobility of graphene, the photo-induced electrons could be exported via graphene sheets, which effectively separated the electrons and holes and reduced the recombination rate. That was to say, more photo-induced holes and hydroxyl radical involved in the photocatalytic process, and the photocatalytic efficiency of the composite enhanced significantly.

Conclusion

It is an effective route to obtain a ZnO/graphene composite with high photocatalytic properties via high temperature treatment since during the process of Zn transformed into ZnO, a tight contact heterojunction was formed between ZnO and graphene which greatly improved the separation efficiency of photo-induced electron-holes. The process was simple, economic, and suitable for large quantity preparation. It is applicable in the field of photocatalysis, solar cells, and supercapacitors. With the same principle, the heterojunction of other composite systems, such as, ZnO/TiO_2, ZnO/NiO, ZnO/CuO etc., can also be obtained, and their chemical and physical properties can be further improved.

References

1. Zhang JT, Xiong ZG, Zhao XS (2011) Graphene-metal-oxide composites for the degradation of dyes under visible light irradiation. J Mater Chem 21:3634
2. Zhang YP, Cao B, Zhang B, Qi X, Pan CX (2012) The production of nitrogen-doped graphene from mixed amine plus ethanol flames. Thin Solid Films 520:6850
3. Park WI, Lee CH, Lee JM, Kim NJ, Yi GC (2011) Inorganic nanostructures grown on graphene layers. Nanoscale 3:3522
4. Zhang YP, Pan CX (2011) TiO_2/graphene composite from thermal reaction of graphene oxide and its photocatalytic activity in visible light. J Mater Sci 46:2622
5. Williams G, Kamat PV (2009) Graphene-semiconductor nanocomposites: excited-state interactions between ZnO nanoparticles and graphene oxide. Langmuir 25:13869
6. Zhang YP, Li CZ, Pan CX (2012) N + Ni Co doped anatase TiO_2 nanocrystals with exposed {001} facets through two-step hydrothermal route. J Am Ceram Soc 95:2951
7. Zhang YP, Fei LF, Jiang XD, Pan CX, Wang Y (2011) Engineering nanostructured Bi_2WO_6-TiO_2 toward effective utilization of natural light in photocatalysis. J Am Ceram Soc 94:4157
8. Li DL, Pan CX (2012) Fabrication and characterization of electrospun TiO_2/CuS micro-nano-scaled composite fibers. Prog Nat Sci 22:59
9. Li DL, Jiang XD, Zhang YP, Zhang B, Pan CX (2013) A novel route to ZnO/TiO_2 heterojunction composite fibers. J Mater Res 28:507
10. Djurisic AB, Chen XY, Leung YH, Ng A (2012) ZnO nanostructures: growth, properties and applications. J Mater Chem 22:6526
11. Kim YJ, Lee JH, Yi GC (2009) Vertically aligned ZnO nanostructures grown on graphene layers. Appl Phys Lett 95:213101
12. Hwang JO, Lee DH, Kim JY, Han TH, Kim BH, Park M, No K, Kim SO (2011) Vertical ZnO nanowires/graphene hybrids for transparent and flexible field emission. J Mater Chem 21:3432
13. Lin J, Penchev M, Wang GP, Paul RK, Zhong JB, Jing XY, Ozkan M, Ozkan CS (2010) Heterogeneous graphene nanostructures: ZnO nanostructures grown on large-area graphene layers. Small 6:2448

14. Lu T, Pan LK, Li HB, Zhu G, Lv T, Liu XJ, Sun Z, Chen T, Chua DHC (2011) Microwave-assisted synthesis of graphene-ZnO nanocomposite for electrochemical supercapacitors. J Alloy Compd 509:5488

15. Zhang YP, Li HB, Pan LK, Lu T, Sun Z (2009) Capacitive behavior of graphene-ZnO composite film for supercapacitors. J Electroanal Chem 634:68

16. Zheng WT, Ho YM, Tian HW, Wen M, Qi JL, Li YA, Li YA (2009) Field emission from a composite of graphene sheets and ZnO nanowires. J Phys Chem C 113:9164

17. Yin ZY, Wu SX, Zhou XZ, Huang X, Zhang Q, Boey F, Zhang H (2010) Electrochemical deposition of ZnO nanorods on transparent reduced graphene oxide electrodes for hybrid solar cells. Small 6:307

18. Li BJ, Cao HQ (2011) ZnO@graphene composite with enhanced performance for the removal of dye from water. J Mater Chem 21:3346

19. Xu TG, Zhang LW, Cheng HY, Zhu YF (2011) Significantly enhanced photocatalytic performance of ZnO via graphene hybridization and the mechanism study. Appl Catal B-Environ 101:382

20. Guo HL, Wang XF, Qian QY, Wang FB, Xia XH (2009) A green approach to the synthesis of graphene nanosheets. ACS Nano 3:2653

21. Yu W, Pan CX (2009) Low temperature thermal oxidation synthesis of ZnO nanoneedles and the growth mechanism. Mater Chem Phys 115:74

22. Kovtyukhova NI, Ollivier PJ, Martin BR, Mallouk TE, Chizhik SA, Buzaneva EV, Gorchinskiy AD (1999) Layer-by-layer assembly of ultrathin composite films from micron-sized graphite oxide sheets and polycations. Chem Mater 11:771

23. Hirakawa T, Nosaka Y (2002) Properties of $O_2^{\bullet-}$ and OH• formed in TiO_2 aqueous suspensions by photocatalytic reaction and the influence of H_2O_2 and some ions. Langmuir 18:3247

24. Jiang XD, Shi AQ, Wang YQ, Li YZ, Pan CX (2011) Effect of surface microstructure of TiO_2 film from micro-arc oxidation on its photocatalytic activity: a HRTEM study. Nanoscale 3:3573

25. Kashif M, Ali S, Ali ME, Abdulgafour HI, Hashim H, Willander M, Hassan Z (2012) Morphological, optical, and raman characteristics of ZnO nanoflakes prepared via a sol-gel method. Phys Status Solidi A 209:143

26. Brandes EA, Brook GB (1992) Smithells metals reference book, vol 13, 7th edn. Butterworth-Heinemann, Oxford

27. Ren ZS, Hu XJ, Xue XX, Chou KC (2013) Solid state reaction studies in Fe_3O_4–TiO_2 system by diffusion couple method. J Alloy Comp 580:182